



Vulnerability to forest loss through altered postfire recovery dynamics in a warming climate in the Klamath Mountains

Alan J. Tepley¹  | Jonathan R. Thompson² | Howard E. Epstein³ |
Kristina J. Anderson-Teixeira^{1,4} 

¹Smithsonian Conservation Biology Institute, Front Royal, VA, USA

²Harvard Forest, Petersham, MA, USA

³Department of Environmental Sciences, University of Virginia, Charlottesville, VA, USA

⁴Center for Tropical Forest Science – Forest Global Earth Observatory, Smithsonian Tropical Research Institute, Panama, Republic of Panama

Correspondence

Alan Tepley, Smithsonian Conservation Biology Institute, Front Royal, VA, USA.
Email: TepleyA@si.edu

Funding information

National Science Foundation, Grant/Award Number: DEB-1353301

Abstract

In the context of ongoing climatic warming, certain landscapes could be near a tipping point where relatively small changes to their fire regimes or their postfire forest recovery dynamics could bring about extensive forest loss, with associated effects on biodiversity and carbon-cycle feedbacks to climate change. Such concerns are particularly valid in the Klamath Region of northern California and southwestern Oregon, where severe fire initially converts montane conifer forests to systems dominated by broadleaf trees and shrubs. Conifers eventually overtop the competing vegetation, but until they do, these systems could be perpetuated by a cycle of reburning. To assess the vulnerability of conifer forests to increased fire activity and altered forest recovery dynamics in a warmer, drier climate, we characterized vegetation dynamics following severe fire in nine fire years over the last three decades across the climatic aridity gradient of montane conifer forests. Postfire conifer recruitment was limited to a narrow window, with 89% of recruitment in the first 4 years, and height growth tended to decrease as the lag between the fire year and the recruitment year increased. Growth reductions at longer lags were more pronounced at drier sites, where conifers comprised a smaller portion of live woody biomass. An interaction between seed-source availability and climatic aridity drove substantial variation in the density of regenerating conifers. With increasing climatic water deficit, higher propagule pressure (i.e., smaller patch sizes for high-severity fire) was needed to support a given conifer seedling density, which implies that projected future increases in aridity could limit postfire regeneration across a growing portion of the landscape. Under a more severe prospective warming scenario, by the end of the century more than half of the area currently capable of supporting montane conifer forest could become subject to minimal conifer regeneration in even moderate-sized (10s of ha) high-severity patches.

KEYWORDS

Douglas-fir, forest resilience, Klamath Mountains, postfire recruitment, propagule pressure, reburn, stem analysis, tipping point, tree regeneration

1 | INTRODUCTION

Vegetation dynamics shortly after forest disturbances have long-lasting effects on stand development and the variation in forest composition and structure across landscapes (Turner, Dale, & Everham, 1997). In the case of fire, both the disturbance process and the post-disturbance recovery trajectories are subject to modification in a warming climate (Abatzoglou & Williams, 2016; Anderson-Teixeira et al., 2013; Rother, Veblen, & Furman, 2015). Some forest systems may be relatively resilient, in that they can absorb substantial variation in fire frequency, patch sizes, or recovery rates without losing the potential to return to prefire conditions or undergoing dramatic change in the representation of different development stages across the landscapes (Tepley, Swanson, & Spies, 2014). Others may be near a tipping point where relatively small changes to the fire regime or their postfire recovery dynamics could produce extensive and near-irreversible landscape change (Holz, Wood, Veblen, & Bowman, 2015; Tepley, Veblen, Perry, Stewart, & Naficy, 2016). Despite growing insight into altered forest dynamics in a warming climate (Allen, Breshears, & McDowell, 2015; Dobrowski et al., 2015), our understanding of the factors conferring vulnerability and resilience to landscape transformation in the face of climate-altered fire regimes and postfire recovery trajectories is insufficient to assess which systems are closest to a tipping point (Harris, Remenyi, Williamson, Bindoff, & Bowman, 2016).

Forest systems with positive fire–vegetation feedbacks—that is, where the early-seral vegetation that develops after severe fire is either more likely to burn or prone to burn severely than mature forests—may be particularly vulnerable to forest loss through alterations of their fire regimes and forest recovery dynamics (Paritsis, Veblen, & Holz, 2015; Whitlock et al., 2015). A key factor affecting their vulnerability is the rate at which forests recover after severe fire (Tepley et al., 2016). If the duration of the fire-prone, early-seral stage becomes sufficiently long relative to typical intervals between high-severity fires (e.g., due to increasing fire frequency or a slowing of forest recovery), there is potential to perpetuate the nonforest vegetation through a cycle of repeated burning, even where the climate remains suitable to sustain mature forests in the absence of severe fire.

In the western United States, climate change-driven increases in aridity and fire activity (Abatzoglou & Williams, 2016; Barbero, Abatzoglou, Larkin, Kolden, & Stocks, 2015; Diffenbaugh, Swain, & Touma, 2015) might already be altering the trajectories and rates of postfire forest recovery, with the effects likely to become more pronounced in the coming decades. Regardless of future precipitation patterns, which remain uncertain, rising temperatures are likely to drive increasing drought stress across many western forest landscapes due to increasing evapotranspiration, temperature-induced increases in evaporative demand, and reduced winter snowpack (Adams et al., 2009; Gergel, Nijssen, Abatzoglou, Lettenmaier, & Stumbaugh, 2017; Williams et al., 2012). The drier sites within a region currently tend to face greater risk of poor postfire tree recruitment (Dodson & Root, 2013; Donato, Harvey, & Turner,

2016; Rother & Veblen, 2016), suggesting that a growing portion of the landscape could become subject slower forest recovery in a warmer, drier climate. Also, long distance from seed sources, which is commonly associated with larger or more severe fires, can further limit postfire recruitment and extend the time to forest recovery (Donato, Fontaine, Campbell et al., 2009; Harvey, Donato, & Turner, 2016; Kemp, Higuera, & Morgan, 2016).

The Klamath Region of northwestern California and southwestern Oregon is predicted to grow increasingly drought-prone (Diffenbaugh et al., 2015; Swain, Horton, Singh, & Diffenbaugh, 2016) and subject to an increasing frequency of large fires as the climate continues to warm (Barbero et al., 2015; Rogers et al., 2011; Westerling & Bryant, 2008). However, the proximity to a tipping point where such changes could bring about extensive forest loss is not known. Wildfires have burned 25% of the landscape in the last three decades, with 33% of that area having burned at high severity (based on a regionally calibrated threshold of $RdNBR > 574$; Miller et al., 2009). Severe fire initially converts the mixed-conifer and mixed-evergreen forests of the region to an early-seral vegetation dominated by broadleaf trees and shrubs. Conifers commonly show abundant postfire recruitment (Donato, Fontaine, Campbell et al., 2009; Shatford, Hibbs, & Puettmann, 2007) and gradually grow to overtop the competing vegetation. Until they do, however, the early-seral vegetation may be prone to reburn severely, which could repeatedly reset the recovery process until the fire-free interval is eventually sufficient to re-establish a canopy of mature conifers (Odion, Moritz, & DellaSala, 2010; Thompson & Spies, 2010).

Here, we characterize forest recovery dynamics following severe fire in the Klamath Mountains to identify the factors that promote vulnerability and resilience to forest loss in a warming, increasingly arid climate. We sample postfire vegetation across a matrix of climatic water deficit and time-since-fire and pose the following questions: (i) What is the intensity of competition faced by regenerating conifers in the postfire environment? (ii) To what degree does competing vegetation limit the window available for postfire conifer recruitment? (iii) Does early establishment confer a competitive advantage relative to seedlings that establish after the competing vegetation has become dense? and (iv) How do climatic aridity and seed-source variability interact to influence the density of regenerating conifers after fire, and in what ways are those interactions likely to affect the vulnerability to forest loss with increased fire activity in a warmer, drier climate?

2 | MATERIALS AND METHODS

2.1 | Study area

The Klamath Region is characterized by high topographic relief and steep climatic gradients. The climate is Mediterranean, with <15% of annual precipitation falling between May and September. The 37,500-km² region was delineated following the United States Forest Service (USFS) physiographic provinces for the Northwest Forest Plan area (<http://www.reo.gov/maps>) and limited to the area north

of 40°N latitude (Figure 1). Just over half (54%) of the land area is administered by the USFS. We focused on mixed-conifer and mixed-evergreen forests following the BioPhysical Settings of LANDFIRE (NatureServe, 2009). These forest types comprise 74% of the study region (82% of the USFS land), and they occupy a wide aridity gradient. Mean annual precipitation spans an interquartile range of 1,291–2,283 mm (mean 1,855 mm) across their extent on USFS land (<http://prism.oregonstate.edu/>).

Throughout the montane zone, Douglas-fir (*Pseudotsuga menziesii*) dominates the mixed-evergreen forests, and it typically dominates mixed-conifer forests along with one or more of the following species: white fir (*Abies concolor*), incense-cedar (*Calocedrus decurrens*), ponderosa pine (*Pinus ponderosa*), and sugar pine (*Pinus lambertiana*) (Skinner, Taylor, & Agee, 2006). White fir increases in dominance in wetter, upper montane forests. Ponderosa pine becomes increasingly abundant in drier sites and toward the eastern part of the region. The serotinous knobcone pine (*Pinus attenuata*) has a patchy distribution, where it is absent from much of the landscape, but it may be abundant in small patches. The most common broadleaf tree species are tanoak (*Notholithocarpus densiflorus*), madrone (*Arbutus menziesii*), chinkapin (*Chrysolepis chrysophylla*), and canyon live oak (*Quercus chrysolepis*), all of which resprout prolifically from the root collar when topkilled by fire (Donato, Fontaine, Robinson, Kauffman, & Law, 2009). Shrub species of two genera, *Ceanothus* and *Arctostaphylos*, exhibit abundant postfire recruitment from

a persistent dormant seedbank (Knapp, Weatherspoon, & Skinner, 2012).

2.2 | Field methods

Sample sites were distributed along gradients of time-since-fire and climatic aridity. We represented aridity by the mean annual climatic water deficit, which we calculated following Lutz, van Wagtenonk, and Franklin (2010) using 800-m resolution, 30-year (1981–2010) normals for monthly precipitation and average maximum and minimum monthly temperature (<http://prism.oregonstate.edu/>), and 10-m resolution data on topography and soil water-holding capacity. Water-balance calculations under the Lutz et al. (2010) method retain the high resolution of the soil and topography inputs when they are combined with the coarser gridded climate data.

The area available for sampling was limited to areas <2 km from the nearest road on USFS land, excluding Wilderness Areas and other protected areas, and areas on serpentine bedrock. Candidate sample sites were also limited to areas that burned at high-severity between 1985 and 2009 and had mature conifers present prior to the fire. High burn severity was identified by applying a regionally calibrated RdNBR threshold (>574; Miller et al., 2009). We excluded patches that had burned within a 30-year window prior to the most recent fire to reduce possible influences of short-interval fires (Donato, Fontaine, Robinson et al., 2009). Also, we excluded areas

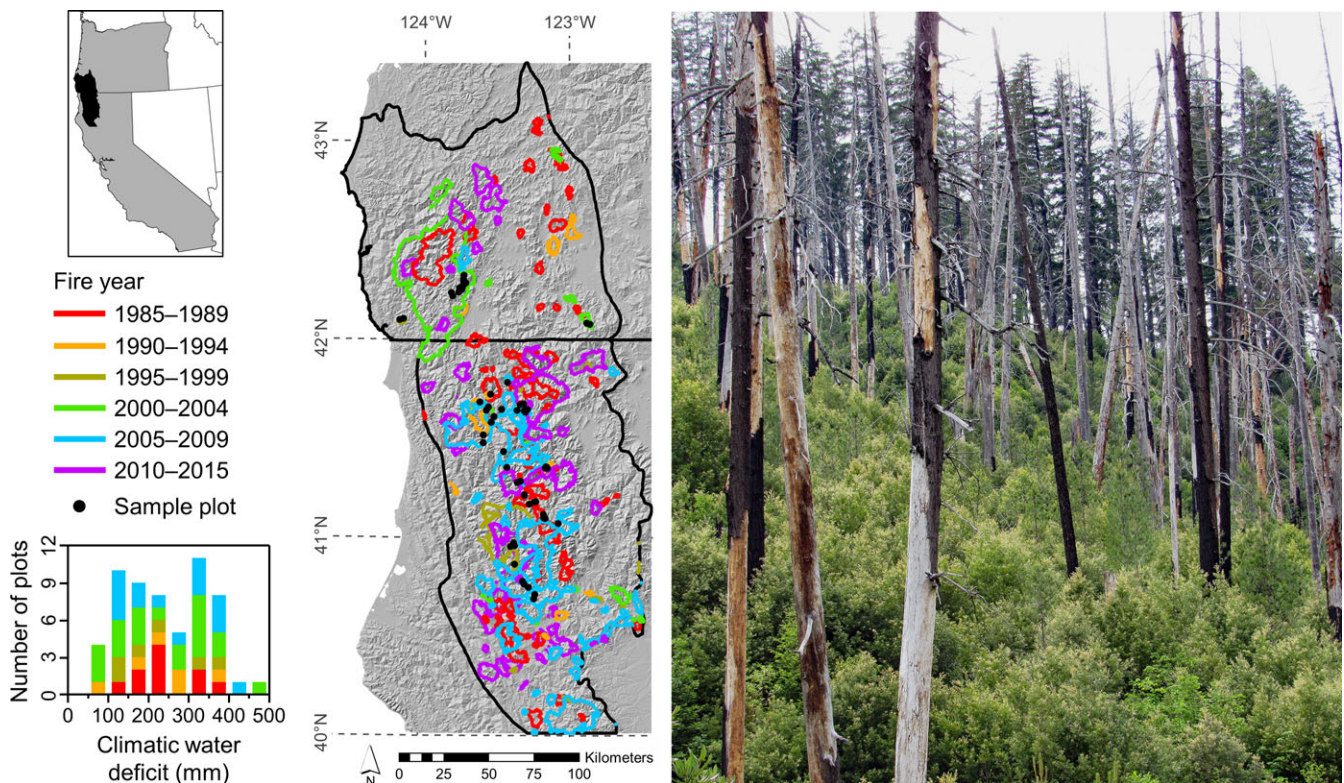


FIGURE 1 Locations of sample plots in the Klamath Mountains in relation to recent fire history (<http://mtbs.gov>). The distribution of mean annual climatic water-deficit values across plots and 5-year time-since-fire bins is shown at lower left. The photograph at right shows the charred conifer snags that formerly dominated the forest and the nearly continuous cover of broadleaf trees and shrubs that persists 21 years after fire, illustrating the characteristic pattern following high-severity fire in the Klamath Region

that had been harvested prior to the fire or had postfire salvage logging or seedling planting, where management history was determined using the Forest Activity Tracker System (FACTS) database for each National Forest. For fires that predate the 20-year FACTS record, candidate sites were retained only if aerial photographs revealed that large conifer snags and logs were distributed throughout the stand, indicating a lack of pre- or postfire harvesting.

In summer 2015, we sampled 57 plots, representing 9 fire years and 22 fires (Figure 1, Appendix S1). The plots spanned 7–28 years since fire (fire years 1987–2008) and climatic water deficit between 78 and 470 mm. We targeted sampling three plots in each cell of a 5×4 matrix of fire years in five 5-year bins (1985–1989, 1990–1994, 1995–1999, 2000–2004, and 2005–2009) and climatic water deficit in four bins (<150, 151–250, 251–350, and >350 mm), revising as necessary to account for differences in the area available for sampling among the time-since-fire bins and to limit travel time between sites and avoid forest closures due to active wildfires (Appendix S1).

Each sample plot was 0.045 ha (15×30 m). Plots were located randomly within the polygons that met our criteria for sampling by using GIS to generate a random point and then using a GPS receiver to locate that point in the field. The distance to the nearest plot was >1 km for 77% of plots and >500 m for all but two pairs of plots that were sampled in the earliest fire year (1987), where the area available for sampling was limited due to uncertainty about postfire management.

Woody vegetation was sampled in three size classes: overstory (tree species >15 cm diameter at breast height; dbh), small trees (tree species 1.5–15.0 cm dbh), and shrubs/saplings (tree species taller than 50 cm and <1.5 cm dbh and shrub species taller than 50 cm with no upper bound on size). For all size classes, tree species included all conifers plus broadleaf tree species capable of growing >5 m tall (Appendix S2). We sampled overstory trees throughout the plot and small trees and the shrub/sapling layer each in three 5×10 -m subplots. For overstory and small trees, we recorded the dbh of all live and standing dead stems, including each stem >1.5 cm dbh for broadleaf trees with multiple stump sprouts. For live stems (2,550 in all), we recorded the crown class (dominant, codominant, intermediate, or suppressed) and measured the total height and crown base height using a pole marked in 0.25-m increments for trees up to 5 m tall or a laser rangefinder for taller trees. The shrub/sapling layer was sampled by recording the height and crown diameter of each individual rooted in the subplots (15,364 in all). For the shrub/sapling layer, clumps of stems originating from a common root collar were treated as one individual. We measured crown diameter along one axis per plant, selected to represent the average crown diameter after excluding individual leaves or fine branches that extended beyond the area of more continuous foliage cover.

At 45 plots, we harvested a subset of the regenerating conifers to determine recruitment dates and reconstruct their height growth via stem analysis. The other 12 plots either lacked regenerating conifers or their climatic water deficit was similar to that of another plot that was destructively sampled within the same fire. Sampling was

limited to Douglas-fir and white fir, which comprised 95% of the regenerating conifers.

Harvesting was conducted within a 200-m radius surrounding the plot to disperse the impact, while selecting individuals in similar competitive environments to those in the plot. We targeted 30 individuals per plot with the number harvested in each size class proportionate to that recorded in the plot. Specifically, after sampling vegetation structure, we determined the subset to be harvested by tallying the trees recorded in the following size classes: greater than or less than 1-m tall for the shrub/sapling layer, and 1.5–3.0, 3.0–5.0, and >5.0 cm dbh for the small-tree layer. Although sampling of the shrub-sapling layer was limited to plants taller than 50 cm, seedlings shorter than 50 cm were harvested where present. Fewer than 30 trees were sampled where the density of postfire conifers was particularly low. Altogether, 1,178 conifers were harvested (mean 26 per plot), with heights ranging from 0.15 to 8.88 m. Stems were cut as close to the mineral soil surface as possible, and we recorded the cutting height for each tree. We collected the basal cross section of each tree, plus additional cross sections at each 10-cm interval up to 50 cm, and then at each 25-cm interval to the top of the tallest shoot.

2.3 | Analyses

2.3.1 | Postfire competitive environment

To characterize the competitive environment faced by regenerating conifers, we evaluated trends in aboveground live woody biomass with time-since-fire for three physiognomic groups: conifers, broadleaf trees, and shrubs. Biomass for 11 of the 15 species (67% of stems) recorded in the small-tree layer and 37 of 63 species (94% of individuals) in the shrub/sapling layer was estimated using genus- or species-specific allometry (Appendix S2). For the remaining species, we used either an equation from another species of similar form or a composite equation developed from several species common to the region (McGinnis, Shook, & Keeley, 2010).

Trends in biomass with time-since-fire were fit with Generalized Additive Models (GAMs) using the R package “mgcv” (R Core Team, 2016; Wood, 2011). We fit one model for each physiognomic group using a cubic regression spline as the smoothing function. Before fitting the models, we removed outliers that were more than two standard deviations from the mean biomass of the respective group within a 5-year time-since-fire window. Also, to reduce the trend of increasing variance with time-since-fire, we transformed the biomass values as $\sqrt{x_{ij} + 0.5}$, where x_{ij} is the biomass of the j^{th} physiognomic group in the i^{th} plot (Yamamura, 1999). To assess the proportion of variance in each group explained by climatic aridity after accounting for trends with time-since-fire, we used linear regression to relate the GAM residuals to climatic water deficit.

2.3.2 | Conifer recruitment and growth

To evaluate conifer recruitment and height growth, we determined pith dates for each stem cross section from the harvested trees.

Dating was conducted after sanding until cell structure was visible, using a stereo-zoom microscope. To improve dating accuracy, we identified marker rings that were consistently narrow or wide among individuals, and we compared ring-width patterns at multiple heights along the stem to ensure that we identified extremely narrow or locally absent rings in the most suppressed seedlings. However, the ring-width series were too short (75% of individuals were ≤ 15 years old) for quantitative evaluation of cross-dating accuracy (Grissino-Mayer, 2001).

Analyses were limited to trees for which the basal cross section was cut within 5 cm of the mineral soil surface or those cut at >5 cm and dated to the first year after the fire. These criteria resulted in 1,073 Douglas-fir and 73 white fir trees. All white fir and 92% of Douglas-fir trees were cut within 2 cm of the soil surface (99% and 89%, respectively, within 1 cm). Trees cut at 3–5 cm were primarily from fires of the 1980s and 1990s, and their large sizes made it difficult to cut closer to ground level. Although these basal cross sections could have missed the actual recruitment year, initial growth rates were fast enough that such errors were likely minimal. For instance, of those trees cut within 1 cm of the soil surface, the pith date at 10 cm was the same year or only one year later than the basal cross section in 59% of samples.

We used stem analysis to reconstruct the height growth of Douglas-fir (95% of harvested trees). Heights were estimated for each year up to 2014 (the last complete year of growth). When terminal bud scars were visible and the pith year differed from the sample below it (typically limited to the most recent 3–5 years), we recorded the height of the bud scar as the height at the top of that year's growth. Otherwise, we applied Carmean's (1972) method to estimate the height at the top of each year of growth. This method assumes that sample heights fall at the middle of the year's growth and growth is constant between consecutive samples. It was the most accurate of six methods for estimating true heights from stem analysis data (Dyer & Bailey, 1987).

We evaluated height growth in relation to postfire lags in recruitment to assess the degree to which early recruitment confers a competitive advantage over seedlings that establish later. We defined recruitment lag as the difference between the recruitment year and the fire year, such that seedlings that established the first year after fire had a lag of 1 and those that established the second year had a lag of 2, etc. Height growth was modeled using nonlinear mixed-effects models in the R package "nlme" (Pinheiro, Bates, DebRoy, & Sarkar, 2016). Each model used recruitment lag as a fixed effect, with random effects for each tree nested within its respective plot. Due to decreasing sample size with increasing recruitment lag, we divided recruitment lags into seven bins of increasing size: 1, 2, 3, 4, 5–6, 7–9, and >9 years since fire.

We fit four sigmoidal growth models, including three asymptotic models—logistic, Gompertz, and Chapman-Richards (using functions "SSlogis" and "SSgompertz" in the R "STATS" package and "SSposnegRichards" in the "FlexParamCurve" package; Oswald, Nisbet, Chiaradia, & Arnold, 2012; R Core Team, 2016)—and a nonasymptotic model (Bontemps & Duplat, 2012). The logistic and Gompertz

models each have three parameters, but they differ in that the Gompertz model is not symmetrical around the inflection point. The other two models have four parameters, which provides greater flexibility at the expense of increasing the likelihood that the models will fail to converge to a stable parameterization. To improve the chance of reaching a stable model, we removed trees collected in fire years after 2002, assuming they were too young for growth parameter estimation. Also, we excluded plots from which <18 Douglas-fir trees were sampled to better account for the random effect of tree nested within plot. Models were fit to the remaining data (672 trees in 25 plots) after subsetting the data to even-numbered ages to better emphasize long-term trends as opposed to year-to-year variation.

For the models with stable parameterizations, we used the Akaike information criterion (AIC) to compare fit across different growth models and for different parameterizations within each growth model (i.e., specifying fixed and random effects for different parameters of the growth equation). For the best model (lowest AIC), we used a likelihood ratio test to determine the significance of recruitment lag compared to a model of the same structure but excluding the fixed effect for recruitment lag. Model fit was evaluated by the mean absolute error (MAE) and the modified coefficient of efficiency (E_1), where $E_1 = 1$ represents a perfect fit and $E_1 = 0$ indicates model predictions are no better than the observed mean (Legates & McCabe, 1999, 2013). We also solved the fitted growth equations to determine the maximum annual growth for each of the seven recruitment lag bins.

To further evaluate relationships between height growth and recruitment lag, we assessed whether the height at each age (1–15 years) differed among the seven recruitment lag bins using linear mixed-effects models in the R package "lme4" (Bates, Mächler, Bolker, & Walker, 2015). Constructing a separate model for each age rather than modeling the growth of each tree, as in the previous analysis, enabled us to use linear models with a single random effect for plot instead of nested random effects for tree within plot. This simpler model construction breaks up the longitudinal data, but it allows for more explicit quantification of the variance explained by the fixed factor (recruitment lag) alone and that explained by both fixed and random effects using the marginal and conditional R^2 (R_M^2 and R_C^2 , respectively) of Nakagawa and Schielzeth (2013). Also, because we developed a separate model for each age rather than fitting growth curves, young trees no longer presented a problem for parameter estimation, so we included all plots with >18 Douglas-fir trees regardless of the fire year (970 trees in 35 plots).

For each age in which height differed significantly by recruitment lag, we evaluated whether trees that established at each lag >1 year were significantly shorter than trees that established the first year after fire using a one-sided Dunnett's test (Hsu, 1996) in the R package "multcomp" (Hothorn, Bretz, & Westfall, 2008). This test treats lag 1 as a control group and each subsequent lag as a separate treatment. We used a one-sided test because we were interested specifically in whether longer lags led to shorter height for a given age.

2.3.3 | Drivers of conifer recruitment density

Recent studies identify two key drivers of the postfire density of regenerating conifers: seed-source availability and climatic aridity (Donato et al., 2016; Harvey et al., 2016; Kemp et al., 2016; Rother & Veblen, 2016). We represented climatic aridity using the mean annual climatic water deficit. To represent seed-source availability, we developed a proxy for propagule pressure, which we defined as the proportion of the area within a 400-m radius circle (50 ha) centered on each plot that supports mature conifers that survived the fire. We chose this approach because the mixed-severity fires characteristic of the Klamath Region leave surviving trees in varying patterns and densities (Halofsky et al., 2011), where distance to the nearest seed source might poorly represent the ways that different live-tree patch sizes and configurations affect seed distribution. We chose a 400-m radius based on a study following the 2002 Biscuit Fire, in which conifer seedling density remained high up to 400 m from seed sources but decreased abruptly thereafter (Donato, Fontaine, Campbell et al., 2009). The circle serves as the source area from which the majority of seeds that dispersed into our plot were likely to have originated. To quantify propagule pressure for each plot, we overlaid a grid of 10 × 10-m cells on the 50-ha circle surrounding each severely burned plot and used aerial photographs to label cells as supporting seed sources if the crowns of mature conifer trees comprised at least half of the cell area.

We evaluated how propagule pressure and climatic water deficit interact to drive variation in the initial density of regenerating conifers following severe fire using Non-Parametric Multiplicative Regression (NPMR; McCune, 2006) in HYPERNICHE 2.30 (McCune & Mefford, 2009). NPMR identifies thresholds with little sensitivity to their magnitude or the nature of the interactions between predictors (Lintz, McCune, Gray, & McCulloh, 2011). The response at each sample plot is estimated as the weighted mean of the responses across all other plots, where the weight for each plot is the product of its weights for the two predictors (McCune, 2006). For each predictor, a plot with the same value as the target plot is assigned a weight of 1, and the rate at which weights decrease with increasing difference from the target is tuned by adjusting the standard deviation of a Gaussian kernel centered on the target plot. When a sample plot is far from the target plot in one of the predictors, its weight for that predictor will be near zero, and the plot will have minimal influence on the estimated response regardless of its weight for the other predictor. In this way, responses may vary markedly in different portions of the predictor gradient.

We constructed two NPMR models. The first used the density of regenerating conifers (excluding the serotinous knobcone pine) as a continuous response variable. Conifer density was transformed following the generalized log transformation described in McCune and Grace (2002; p. 69), which tends to preserve the order of magnitude in the data while retaining zero values. Because our plots span 7–28 years since fire, variation in conifer density among plots could be driven in part by the different windows available for recruitment and mortality. Therefore, the second version of the model used the

probability of nonserotinous conifers exceeding a minimum stocking density as a binary response that is less likely to be influenced by varying time-since-fire.

For the binary model, we used a threshold seedling density of 340 ha⁻¹ to approximate whether stands were on a trajectory toward forest recovery. This value is intermediate between the target minimum stocking level to be reached within 5 year following timber harvest in mixed-conifer (371 ha⁻¹) and Douglas-fir (309 ha⁻¹) forests, as suggested in the Land and Resource Management Plans for the Klamath (USDA, 1995a) and Shasta-Trinity (USDA, 1995b) National Forests. The same values were provided for Site Class III and all other productivity levels, respectively, for the Siskiyou National Forest (USDA, 1989). The Forest Plans also set a higher, recommended stocking level, which would lead to more rapid stand development and eligibility for commercial thinning (USDA, 1995a), but we used the minimum stocking level as a more conservative value that is not as strongly tied to timber management objectives.

NPMR guards against overfitting by excluding the values from each plot when estimating its response, which provides a cross-validated means to quantify model fit (xR^2 for the continuous response; McCune, 2006). Fit of the binary model ($\log B$) was calculated as the ratio of the likelihood of cross-validated estimates from the fitted model to estimates from the naïve model expressed in powers of ten, where the naïve model is the proportion of plots that exceeded the minimum stocking density across our dataset. Statistical significance was evaluated using a Monte Carlo simulation with 999 replications (McCune, 2006).

To illustrate how the interactions uncovered by NPMR could affect postfire conifer recruitment in a warmer, drier climate, we estimated the mean annual climatic water deficit across the Klamath Region for the year 2100 under the 2.6 and 8.5 representative concentration pathways (RCPs). Future deficit values were calculated following Lutz et al. (2010) using the HadGEM2 climate model (Collins et al., 2011; Jones et al., 2011).

We also applied the NPMR models to estimate conifer recruitment across the severely burned portions of two recent fires: the Butler and Salmon River Fires of 2013 (9,729 and 6,049 ha, respectively). These fires are centrally located with respect to our plots, and imagery of the National Agriculture Imagery Program (NAIP) was collected early in the first growing season after the fires, which facilitated identification of remaining seed sources. To calculate propagule pressure, we first applied the Visible Atmospherically Resistant Index (VARI), which was developed to identify green vegetation fraction while reducing atmospheric effects (Gitelson, Kaufman, Stark, & Rundquist, 2002). We applied VARI to the 1-m resolution NAIP imagery for each fire plus a 400-m buffer. We then aggregated to 10-m resolution and subjectively set a threshold as a first approximation of the areas with surviving mature trees. We revised the classification by hand to exclude meadows and improve classification accuracy where needed (e.g., areas with heavy shadows). A propagule pressure layer for the areas lacking surviving canopy was then developed using focal statistics in ArcGIS 10.4 (ESRI, 2015). Finally, we

entered the propagule pressure and climatic water-deficit layers (Lutz et al., 2010) as predictors into our NPMR models to estimate the density of regenerating conifers throughout the severely burned portions of the fires.

3 | RESULTS

3.1 | Postfire competitive environment

Conifers faced a highly competitive environment following severe fire. Woody vegetation regrew rapidly, but conifers averaged only 8% of aboveground live woody biomass over postfire years 7–28 (Figure 2). Although conifers were dominant in a small number of plots (>50% of biomass in 9% of plots), they represented <5% of woody biomass in more than half (53%) of the plots.

Biomass of the three physiognomic groups varied widely among plots (Figure 2a), but trends of increasing biomass with time-since-fire were relatively strong for both conifers ($p < .001$, 33.8% deviance explained) and broadleaf trees ($p < .001$, 43.1% deviance explained). Shrub biomass tended to peak in the second decade and then decline as the shrubs began to become shaded by taller tree species ($p < .01$, 20.9% deviance explained).

Conifers faced an increasingly competitive environment with increasing aridity. Residuals from GAM models of trends in both conifer biomass and the conifer proportion of total live woody biomass with time-since-fire became increasingly negative with increasing climatic water deficit ($R^2 = 0.14$, $p < .01$ for conifer biomass and $R^2 = 0.31$, $p < .001$ for the conifer proportion of total biomass; Appendix S3). This trend may be driven by increasing shrub biomass

in drier sites; residuals from the shrub biomass model were positively correlated with climatic water deficit ($R^2 = 0.07$, $p = .03$), whereas residuals from the model for broadleaf tree species were not significantly related to deficit ($p = .059$).

3.2 | Conifer recruitment and growth

Douglas-fir and white fir were by far the most abundant regenerating conifers. Douglas-fir comprised 64% of individuals and was recorded in 77% of plots, whereas white fir represented 31% of individuals and was recorded in 19% of plots. Five additional conifers (knobcone pine, ponderosa pine, sugar pine, incense-cedar, and western white pine) comprised the remaining 5% of regenerating conifers, and none of these species were found in more than 19% of the plots.

Successful recruitment for Douglas-fir and white fir was limited to a narrow window following severe fire (Figure 3). Overall, 89% of Douglas-fir recruitment dates fell within the first 4 years. Our finding that recruitment was limited to the first few years following the earlier fires (1987–2002) indicates that the interval from the more recent fire years (2006–2008) to our sampling was probably long enough to include nearly the entire pulse of recruitment initiated by the fires (Figure 3a). The proportion of recruitment dates in each year since fire varied among plots and across fire years (Figure 3b), but cumulative recruitment was consistently near 100% within the first few years (median of 96% by the end of the fourth year; Figure 3c). White fir was sampled in fewer plots ($n = 6$), but its recruitment patterns were similar to Douglas-fir. Altogether, 95% of its recruitment dates were recorded within the first 4 years (Figure 3a).

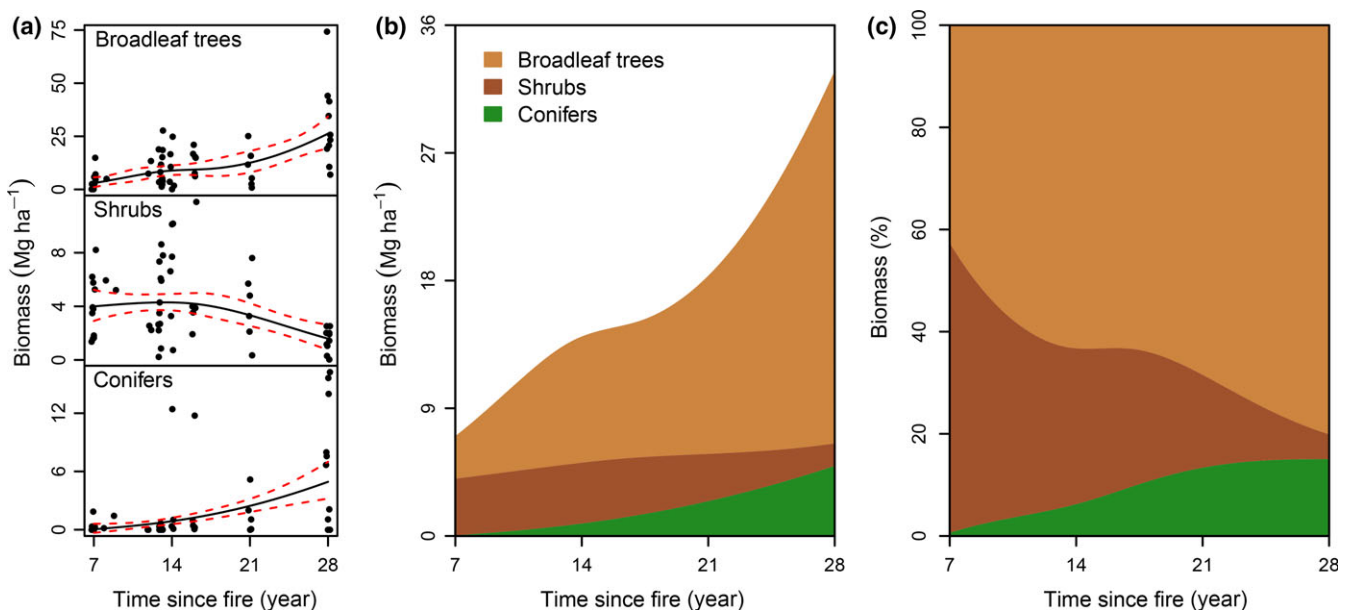


FIGURE 2 Trends in aboveground live woody biomass with time-since-fire for conifers, broadleaf trees, and shrubs. In (a), trends are fit for each physiognomic group using GAMs with a spline smoothing function (solid black curve). Red dashed lines represent standard errors. To reduce overlapping points for visual interpretation, the x-axis values of plots (black dots) are staggered by up to ± 0.2 years. The fitted curves from panel (a) were used to approximate the absolute and relative proportions of total biomass in panels (b) and (c), respectively, represented by each physiognomic group over postfire years 7–28

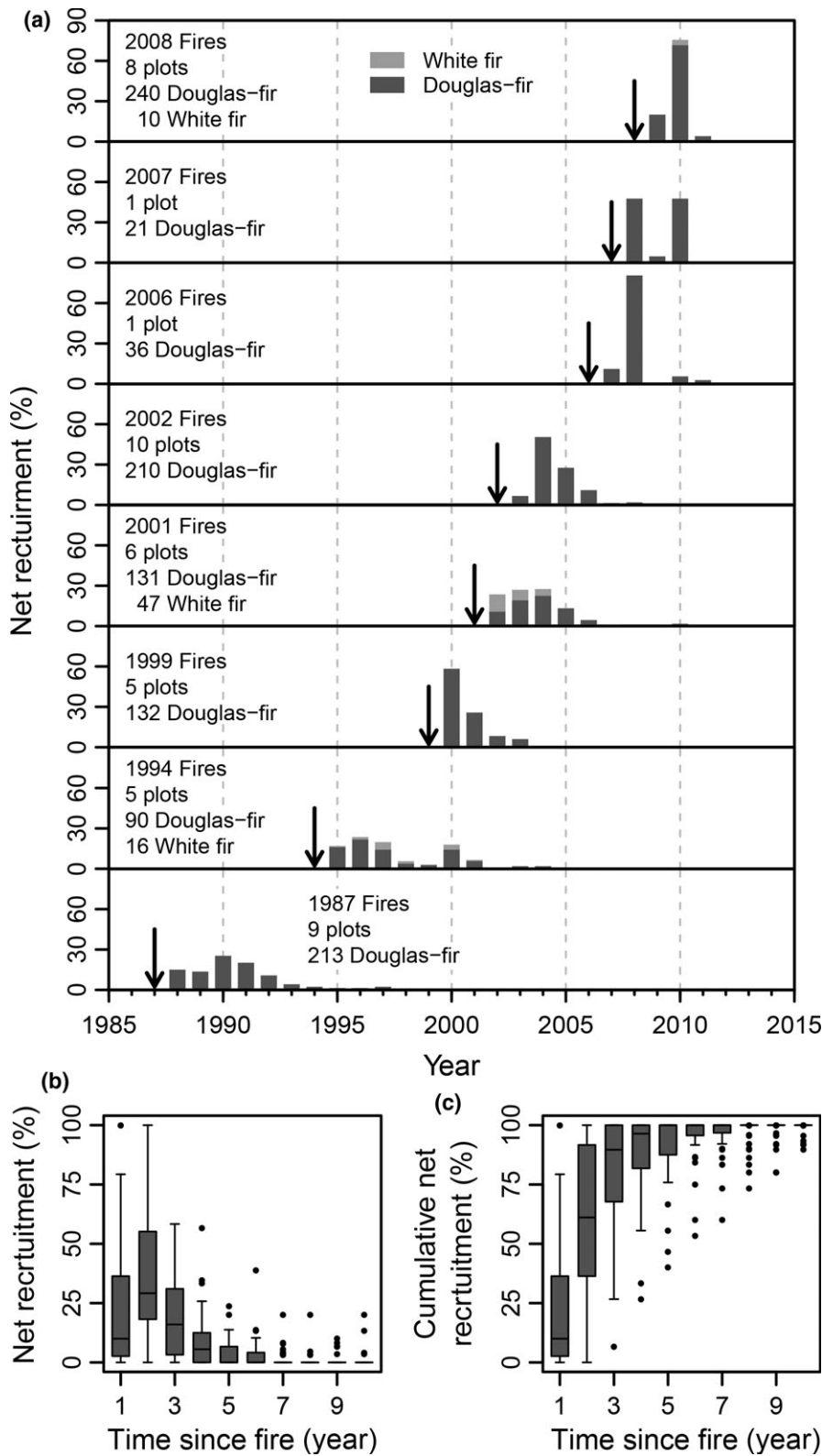


FIGURE 3 Postfire recruitment patterns with time-since-fire. In (a), recruitment for Douglas-fir and white fir is compared across eight fire years, where the arrow indicates the fire year and values are aggregated across plots (no seedlings were present in the two plots sampled in a 2003 fire). For Douglas-fir, box-and-whisker plots illustrate the variation in (b) annual net recruitment (i.e., establishment and survival to the time of sampling) and (c) cumulative net recruitment across plots with time-since-fire

Models of Douglas-fir height growth (Figures 4 and 5) converged to stable solutions for only the logistic and Gompertz models, and the Gompertz model provided a better fit (AIC = 42,467 compared to 45,480 for the logistic model). Our inability to reach stable models for the Chapman-Richards and nonasymptotic sigmoidal models was likely because trees were too young to fit parameters for the

inflection point or the later growth patterns (Figure 4). The best parameterization (lowest AIC) using a Gompertz model had fixed effects for the asymptote and position parameters (*Asym* and *b2* following the notation of the R “SSgompertz” function) for the seven recruitment lag bins, and random effects for the same two parameters for each tree nested within its respective plot. Adding fixed or

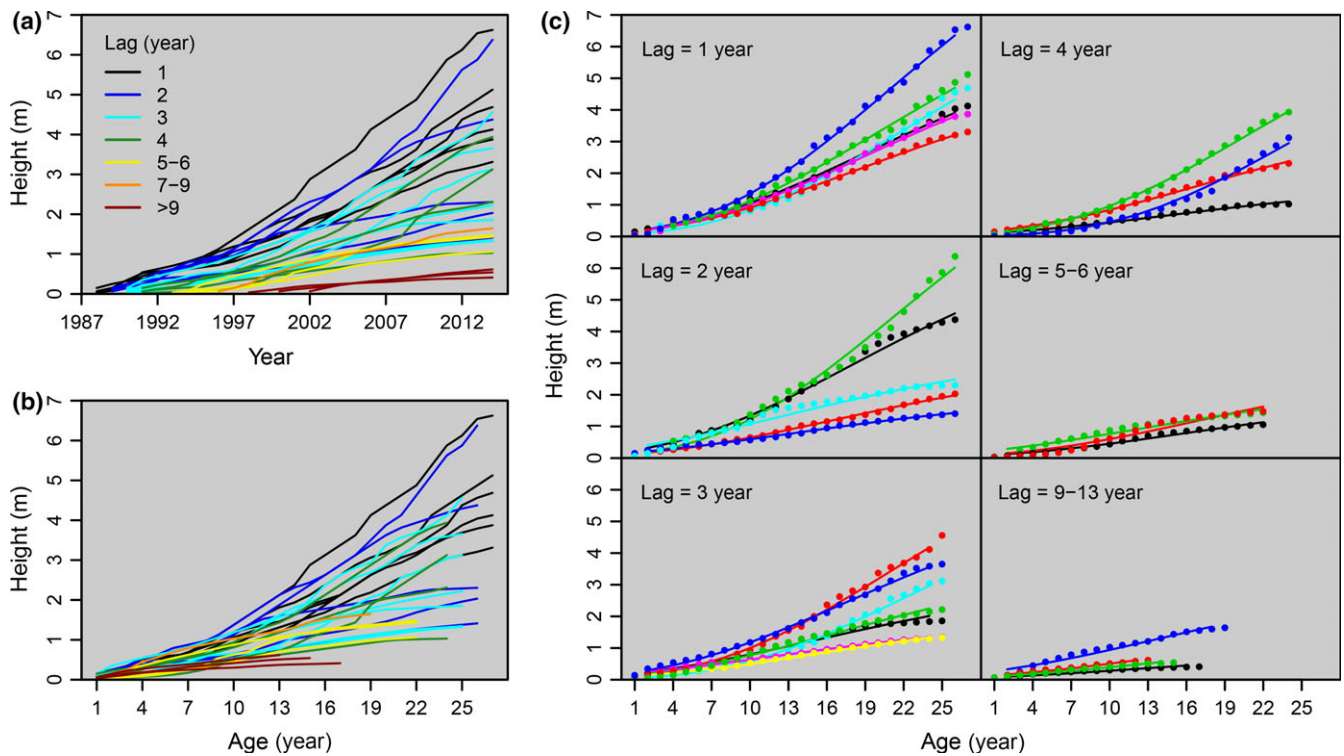


FIGURE 4 Height growth for 29 Douglas-fir trees in a representative plot in the 1987 King Titus Fire (selected because it was the earliest fire year and recruitment dates were represented in all recruitment lag bins). The heights determined by stem analysis are plotted by tree to illustrate (a) the increasing variability in height with time-since-fire, and (b) the variability in growth rates among trees. In (c), the heights at each age (dots) are plotted along with the fitted curves (one color per tree) using the random effects parameters derived from the Gompertz growth model in order to illustrate model fit and the trend of decreasing growth rate with increasing recruitment lag

random effects for the scale parameter (b_3) prevented convergence to a stable model. The effect of recruitment lag was highly significant ($p < .0001$), and model fit was reasonably strong (MAE = 6.6 cm, $E_1 = 0.90$).

Among the regenerating Douglas-fir seedlings, early recruitment conferred a competitive advantage, whereby the shorter the lag between the fire year and the recruitment year, the faster the height growth (Figures 4 and 5). Heights at the time of sampling were highly variable within plots, and taller trees tended to be older than shorter trees (Figure 4a). However, those trees with the earliest recruitment dates also tended to exhibit faster growth throughout their lives than trees with later recruitment (Figure 4b, c). Fitted curves for each recruitment lag bin across the full dataset (672 trees in 25 plots) indicate that trees with lags of 1 and 2 years reached a maximum annual growth of 17.5 cm, whereas trees with lags >9 years had maximum annual growth of only 7.2 cm (Figure 5a).

The reduction in height growth at longer lags was more pronounced at drier sites. When the Gompertz model was reparameterized for data divided into plots with climatic water deficits above and below the median value (218 mm) of the stem analysis dataset (xeric and mesic sites), the maximum annual growth for trees with short recruitment lags differed little between models (14.8 and 16.5 cm for trees of lag 1 on mesic and xeric sites, respectively). However, for trees with lags >9 years, the maximum annual growth on xeric sites (4.1 cm) was less than half that found on mesic sites (8.5 cm).

The variation in Douglas-fir height at each age further elucidates the trend of decreasing height growth with increasing recruitment lag (Figure 5b). Seedlings with a lag of 2 years were not significantly shorter than those of lag 1 at any age. However, seedlings with a lag of 4 years were significantly shorter ($p < .05$) than those of lag 1 from ages 4 to 7, and seedlings with lags of 5–6 and 7–9 years were significantly shorter up to age 11. Differences were most pronounced for seedlings with lags >9 years, which were significantly shorter at all ages. Their mean height at age 11 (55 cm) was 52 cm shorter, or only half the height of seedlings of lag 1 (107 cm) when they were 11 years old. The marginal variance explained by recruitment lag (R_M^2) ranged from 3.0% to 4.8% over ages 3–15 years, and the conditional variance explained by recruitment lag together with the random effect of plot (R_C^2) ranged from 11.0% to 33.2% (Figure 5b). The relatively small portion of variance explained by recruitment lag and the decreasing statistical significance of differences in height from lag 1 with increasing age were due in large part to the small sample sizes at longer lags (Figure 3) and further reductions in sample size with increasing age.

3.3 | Drivers of conifer recruitment density

The density of regenerating nonserotinous conifers was relatively high overall (mean and median of 3,732 and 667 ha^{-1} , respectively). However, almost half (46%) of the plots had densities below the

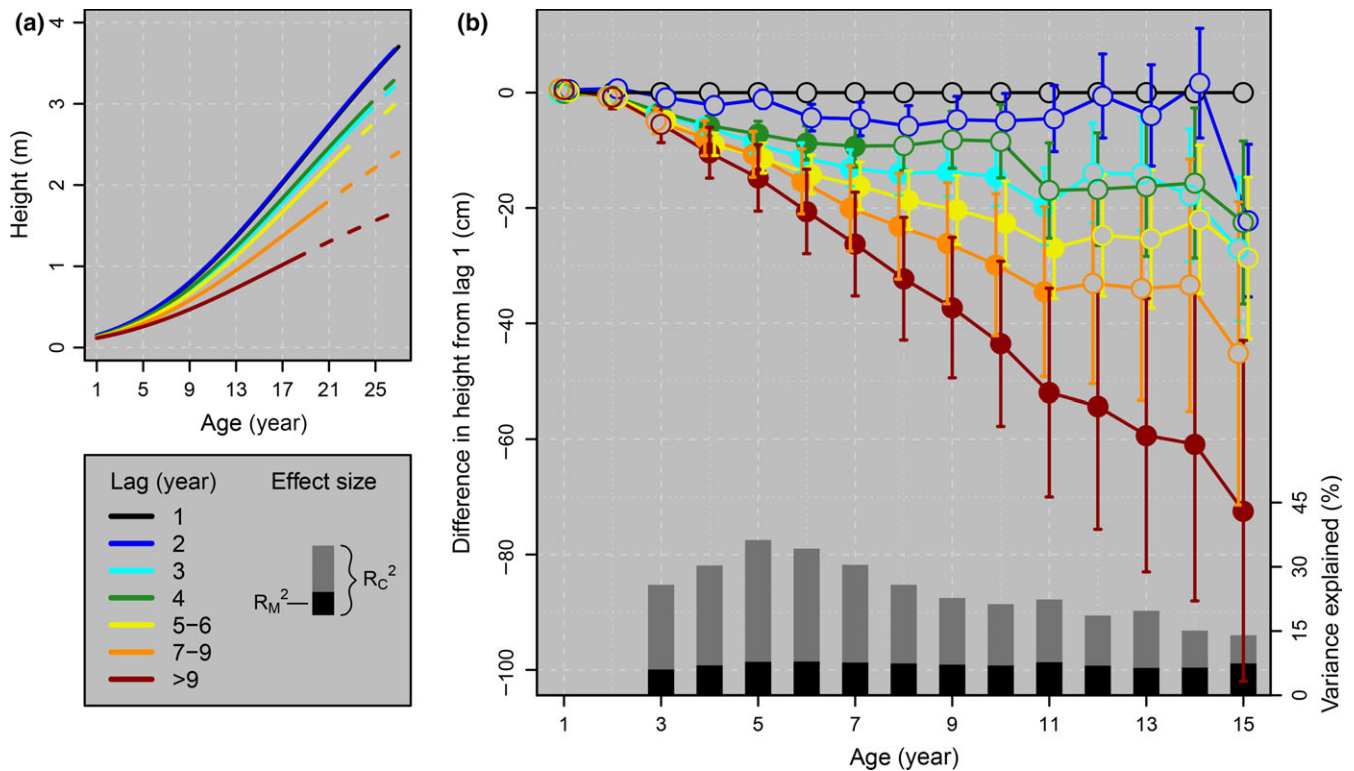


FIGURE 5 Height growth of regenerating Douglas-fir trees following severe fire. In (a), height growth curves are compared among the seven recruitment lag bins using the fixed-effects parameters from the Gompertz growth model for 672 Douglas-fir trees in 25 plots (note that the curves for lags of one and two years are nearly identical). Dashed lines extend beyond the range of ages used to parameterize the model. In (b), the mean height at each age is plotted for 970 Douglas-fir trees in 35 plots in relation to the seven recruitment lag bins. Closed and open circles indicate heights that are significantly shorter ($p < .05$) or not significantly different, respectively, from trees with a lag of one year. Error bars represent the standard error of the mean difference from lag 1. Black and gray bars show the proportion of variance in height explained by the fixed effect of recruitment lag (R_M^2) and by recruitment lag plus the random effect of plot (R_C^2)

minimum stocking level (340 ha^{-1}), and 11 plots (19%) had no regenerating conifers.

An interaction between climatic water deficit and propagule pressure drove a substantial portion of the variation in the density of regenerating conifers following severe fire ($\chi^2 R^2 = 0.41$, $p < .001$; results for the binary model are presented in Appendix S4). With increasing climatic water deficit, higher propagule pressure (i.e., smaller high-severity patch sizes) was needed to maintain a given density of postfire conifer recruitment (Figure 6). The model was equally sensitive to variation in both predictors, with the tolerance equal to 16% of the data range for both variables. Under this tolerance, the weight for a sample plot decreases to 0.5 when propagule pressure differs by 0.14 or climatic water deficit differs by 74 mm from the target plot. The weight decreases to 0.05 when the values differ by 0.28 or 153 mm, respectively.

Based on this statistical model, most of the area currently capable of supporting mixed-conifer/mixed-evergreen forest was predicted to have abundant postfire conifer recruitment except where seed sources were nearly eliminated. However, much of this area could become vulnerable to poor recruitment in a warmer, drier climate (Figure 6). Relatively mesic sites (climatic water deficit $<200 \text{ mm}$) were predicted to have regenerating conifer density well above the minimum stocking level in all but the largest high-severity patches

(propagule pressure <0.2). Deficit values $<200 \text{ mm}$ comprise 59% of the area capable of supporting mixed-conifer/mixed-evergreen forest under recent climate (1981–2010), and 47% of this area is projected to remain at deficits below 200 mm by the end of the century under RCP 2.6. However, areas with climatic water deficit $<200 \text{ mm}$ could decrease to only 22% of the area currently capable of supporting these forest types under RCP 8.5. At climatic water deficit $>300 \text{ mm}$, even small high-severity patches (propagule pressure >0.5) become susceptible to poor postfire recruitment. Although such dry sites comprise only 9% of the area currently capable of supporting mixed-conifer/mixed-evergreen forest, the proportion of this area projected to have deficit $>300 \text{ mm}$ by the end of the century ranges from 16% under RCP 2.6 to 54% under RCP 8.5 (Figure 6).

Application of the NPMR model to the severely burned portions of two recent (2013) fires illustrates how the loss of seed sources over successive fires could limit postfire recruitment (Figure 7). Both fires reburned portions of other recent fires, with 92% of the area burned by the Butler Fire having been burned in 1977 or 2006. Across the Salmon River Fire, 31% of the area burned once within the preceding 36 years, 30% burned twice, and 1% burned three times. The estimated density of regenerating nonserotinous conifers in areas that lacked a surviving tree canopy averaged 828 ha^{-1} (median 384 ha^{-1}) across both fires. However, the estimated seedling

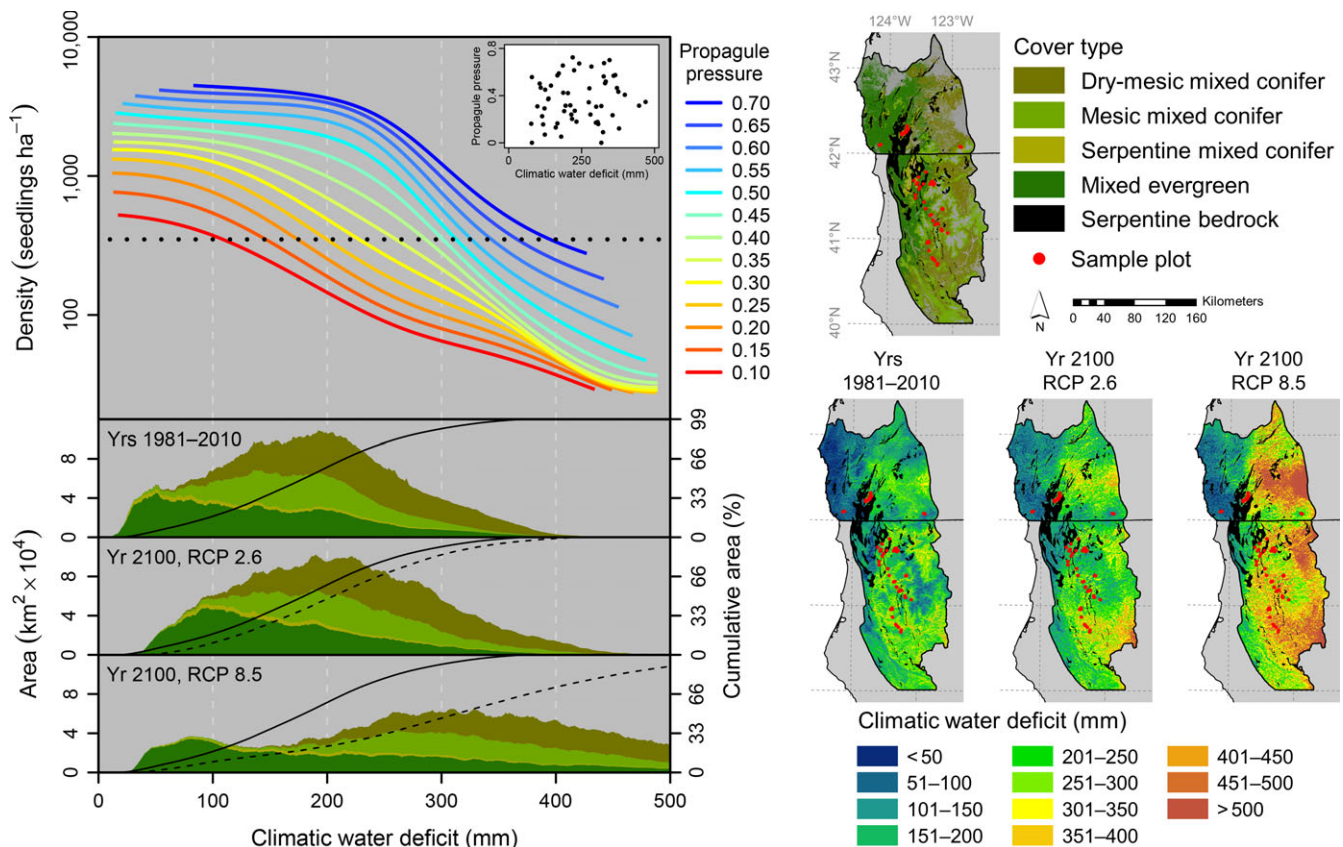


FIGURE 6 Density of regenerating conifers following severe fire, as modeled by the interaction between climatic water deficit and propagule pressure. In the upper-left panel, increasing climatic aridity is represented from left to right along the x-axis, decreasing propagule pressure (i.e., increasing high-severity patch size) is represented from blue to red curves, and the black dotted line represents the minimum stocking density (340 ha^{-1}) recommended in the Forest Plans for three National Forests (USDA, 1989, 1995a,b). The inset graph shows values of the two predictors across our sample plots. Maps show the area capable of supporting mixed-conifer/mixed-evergreen forests (NatureServe, 2009; BioPhysical Setting models 1021, 1022, 1027, 1028, and 1043), and the contemporary (1981–2010) and projected future (yr 2100) climatic water deficit values across the region under RCP 2.6 and 8.5 scenarios. Stacked area graphs (lower left) illustrate the contemporary distribution of deficit values within mixed-conifer/mixed-evergreen forests and the projected future deficit values within areas currently capable of supporting these forest types. The black curves in the lower panels represent the cumulative area within these BioPhysical Settings that falls below a given deficit value under contemporary climate (solid curve) and under the respective future scenario (dashed curve)

density was substantially higher (mean $1,532$, median $1,284 \text{ ha}^{-1}$) where the Butler and Salmon River Fires burned over areas that had not been burned for several decades compared to areas that burned one or more times since the 1970s (mean 697 , median 316 ha^{-1}). This difference can be attributed largely to a loss of seed sources, where propagule pressure in reburned areas (mean 0.22 , median 0.18) was markedly lower than areas that lacked recent fire (mean 0.37 , median 0.43), but climatic water deficit differed little between areas with multiple fires (mean 246 , median 242 mm) and areas without recent fire (mean 220 , median 215 mm ; Figure 7).

4 | DISCUSSION

Our evaluation of forest recovery following severe fire in the Klamath Mountains elucidates how multiple factors interact to confer vulnerability and resilience to forest loss as the climate becomes warmer and more conducive to extensive fire. In response to our

first question concerning the competitive environment faced by conifers regenerating following severe fire, we show that conifers typically comprise only a small portion of the live aboveground biomass for at least the first 28 years (Figure 2). In this highly competitive environment, conifer recruitment was limited primarily to a 4-year window following severe fire, with little variation in the width of that window among fire years (question 2; Figure 3). Furthermore, for Douglas-fir, early-establishing seedlings were at a competitive advantage (question 3), where the height growth decreased as the lag between the fire year and the recruitment year increased (Figures 4, 5). Height growth for seedlings that established at longer lags was more strongly reduced in more arid sites, where seedlings faced an increasingly competitive environment (Appendix S3) and showed more pronounced growth reductions at longer recruitment lags.

With increasing climatic water deficit, higher propagule pressure was needed to support a given density of regenerating conifers (question 4; Figure 6). These results imply that projected increases in aridity (Figure 6; Diffenbaugh et al., 2015) and increases in the

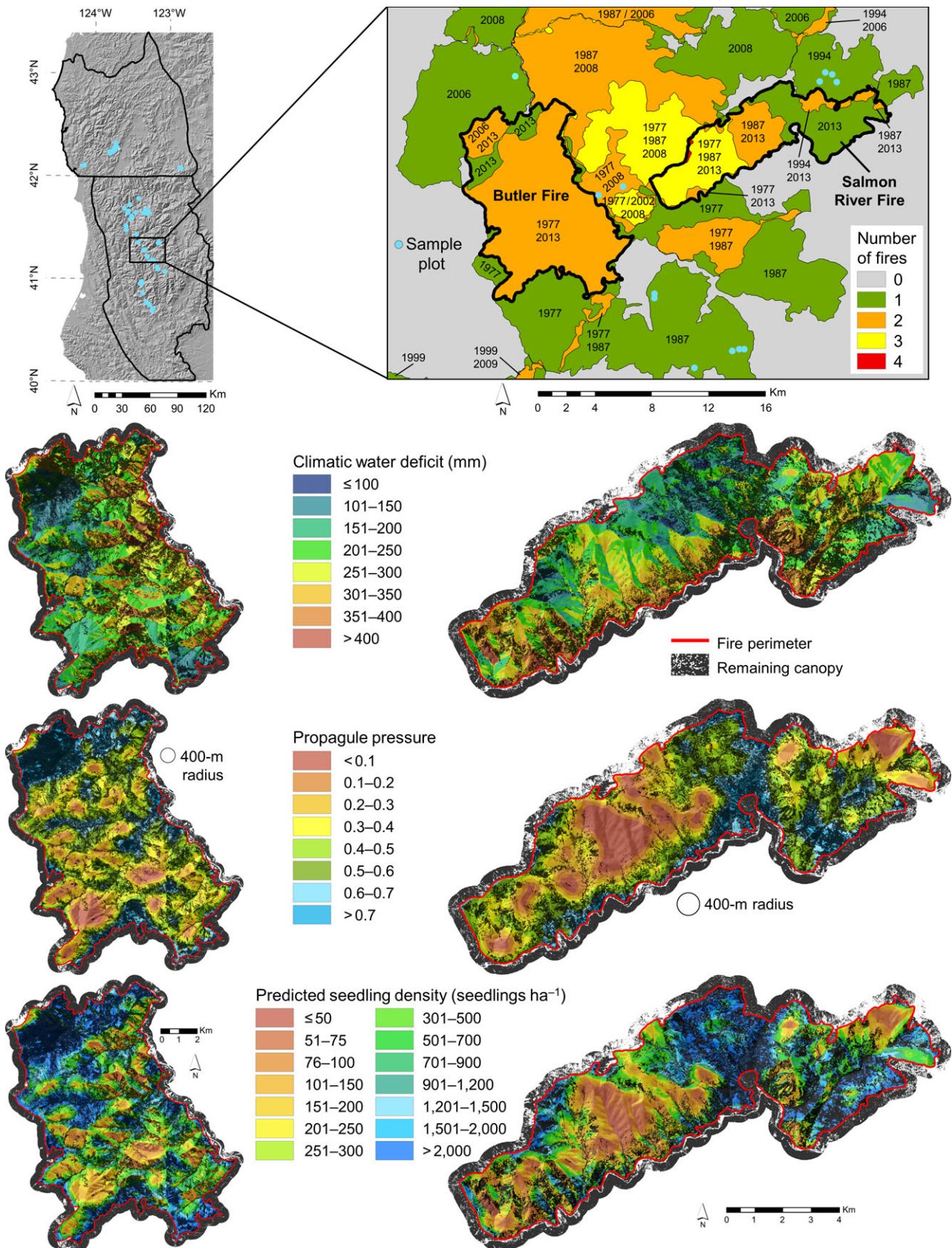


FIGURE 7 Predicted density of regenerating, nonserotinous conifers across portions of the Butler and Salmon River Fires of 2013 (9,079 and 6,049 ha, respectively) that burned severely and lacked a surviving canopy (maps for the binary model are provided in Appendix S4). Maps depict the recent fire history (1977–2013) and the extent of surviving forest canopy along with values for the predictor and response variables across the areas that lacked a surviving canopy after the fires

frequency or extent of severe fire (Abatzoglou & Williams, 2016; Barbero et al., 2015), which increases the potential for areas lacking seed sources to expand over successive fires (Figure 7), could hinder postfire forest recovery over a growing portion of the landscape. Under a more severe warming scenario (RCP 8.5), by the end of the century just over half of the area currently capable of supporting mixed-conifer/mixed-evergreen forests could be at risk of minimal conifer recruitment following severe fire, even in relatively small high-severity patches (Figure 6).

4.1 | Factors promoting resilience

Forests resembling contemporary mixed-conifer/mixed-evergreen forests of the Klamath Mountains developed >2,000 years ago (Briles, Whitlock, & Bartlein, 2005). Their persistence through substantial climatic fluctuation and episodes of frequent fire alternating with longer fire-free intervals and occasional severe events (Colombardi & Gavin, 2010) illustrates a relatively high resilience to variation in the fire regime.

An important factor contributing to that resilience is the topographic complexity of the Klamath Region. Concave features subject to cold-air pooling may remain cooler than predicted by future climate projections (Figure 6) that do not account for fine-scale topographic influences (Daly, Conklin, & Unsworth, 2010). Elevated fuel moisture in these cool microsites could dampen fire severity (Camp, Oliver, Hessburg, & Everett, 1997; Wilkin, Ackerly, & Stephens, 2016), and the surviving trees could facilitate forest recovery by increasing propagule pressure in adjacent, more severely burned areas. Also, an inverse relationship between annual area burned and the proportion burned at high severity has been found for the northern California portion of the region (Miller, Skinner, Safford, Knapp, & Ramirez, 2012), possibly due to a reduction in fire severity under the smoke that accumulates beneath temperature inversions during years of widespread fire (Robock, 1988). Such a mechanism could ameliorate some of the forest loss expected due to climate change-driven increases in fire activity (Abatzoglou & Williams, 2016; Barbero et al., 2015). However, weather largely overrode this mechanism during the 200,000-ha Biscuit Fire (Thompson & Spies, 2010), most of which was excluded from the Miller et al. (2012) analysis.

Douglas-fir was the most abundant regenerating conifer of this and other studies on postfire regeneration in the Klamath Region (Donato, Fontaine, Campbell et al., 2009; Shatford et al., 2007), and its life history and regeneration ecology are conducive to rapid forest recovery following severe fire. The thick bark of mature Douglas-fir enables numerous trees to survive fire as scattered individuals or in patches of varying size and shape (Halofsky et al., 2011). Seed dispersal to at least 400 m from surviving trees promotes high initial postfire seedling density (Donato, Fontaine, Campbell et al., 2009; Donato et al. 2016), except under high climatic water deficit (Figure 6) or where seed sources have been lost in large high-severity patches or over successive burns (Figure 7). By contrast, in drier regions where ponderosa pine is the dominant conifer, postfire seedling density typically decreases to low levels within 200 m of seed

sources (Chambers, Fornwalt, Malone, & Battaglia, 2016; Haire & McGarigal, 2010; Rother & Veblen, 2016). Once established, Douglas-fir seedlings are moderately tolerant to the competitive postfire environment, as illustrated by the enormous plasticity in their early growth (Figures 4, 5; Tepley et al., 2014).

Although the window for successful postfire recruitment was limited to a few years (Figure 3), it was long enough that individual drought years or years of poor seed production were unlikely to be detrimental to forest recovery. For instance, the winter of 2008–2009 was the second driest since 1895 (Palmer Drought Severity Index averaged for CA Division 01 and OR Division 03 for Dec–Jan–Feb = -2.95 ; <http://www7.ncdc.noaa.gov/CDO/CDODivisionalSelect.jsp#>). Recruitment was minimal in 2009 regardless of whether it was the first, second, or third year since fire (Figure 3), suggesting a low winter snowpack may have limited recruitment the following spring. However, for the 2008 fires, six of the eight plots with moderate climatic water deficit (<300 mm) had abundant recruitment in 2010, leading to conifer densities well above the minimum stocking level, although no regenerating conifers were recorded in the four drier plots. With continued warming, climate unfavorable for recruitment could become increasingly common in the first few years following fire. However, future climate projections that do not account for year-to-year variation (Figure 6) might miss the opportunities for successful recruitment when wet years fall within the short window following fire (Serra-Diaz et al., 2016).

Finally, although we did not observe a re-initiation of conifer recruitment since the initial postfire pulse (Figure 3), studies of longer term dynamics suggest conifer forests would eventually recover in the absence of additional fire. In fire-generated chaparral patches of the Sierra Nevada and southern Cascades, conifer recruitment did not peak until 50–70 years after fire, but conifers eventually overtopped the shrubs across much of the burned patches (Lauvaux, Skinner, & Taylor, 2016; Russell, McBride, & Rowntree, 1998). Thus, despite the highly competitive postfire environment and increasing constraints under a warming climate, several features of the Klamath Region ecology ensure that conifer forests will continue to recover following severe fire under moderate increases in climatic aridity, albeit at slower rates or on a reduced portion of the landscape.

4.2 | Factors promoting vulnerability

Despite the factors promoting resilience of mixed-conifer/mixed-evergreen forests of the Klamath Region to a changing climate and fire regime, this study reveals several factors suggesting that drier portions of the region are near a tipping point. If climatic warming drives increases in the frequency and extent of severe fire while causing postfire forest recovery to become increasingly protracted, dry portions of the region could soon exceed a threshold where the intervals between severe fires are rarely sufficient to re-establish forest cover.

Together, the concentration of recruitment dates within similarly short windows among the different fire years (Figure 3), the small portion of aboveground biomass represented by conifers up to at

least 28 years following fire (Figure 2), and the decreasing height growth with increasing recruitment lags (Figures 4, 5) support that biotic competition truncates the initial recruitment pulse following severe fire. Failure to achieve abundant conifer recruitment within the first few years could almost inevitably lead to protracted recovery taking several decades to more than a century to re-establish forest cover (Lauvaux et al., 2016; Russell et al., 1998; Wilken, 1967). This finding is in contrast to the wetter, more productive Douglas-fir/western hemlock forests of the western Cascades of Oregon, where recruitment within a few years and protracted recruitment over several decades were considered endpoints of a continuum of potential trajectories (Tepley et al., 2014). That study used increment cores collected in older forests to evaluate recruitment following historical fires, which provides lower temporal resolution than the seedling ages of the present study. However, differences between regions remained largely consistent when we applied increment coring methods to interpret historical postfire recovery in a small number of older stands in the Klamath Mountains (Appendix S5).

The uniqueness of postfire forest recovery trajectories in the Klamath Mountains is due in part to its unusually high abundance and species diversity of broadleaf trees and shrubs relative to most other conifer forest regions (Skinner et al., 2006). The ability of these species to resprout from an existing root system or germinate from a dormant seedbank (Donato, Fontaine, Robinson et al., 2009; Knapp et al., 2012) pre-positions them to take advantage of the favorable light environment in the first year after severe fire, unlike most conifers that depend on seed dispersal from surviving trees. The potential for the serotinous knobcone pine to facilitate forest recovery in sites beyond the dispersal limit for other conifers may be only locally important. We recorded knobcone pine in only 10 of 57 plots, and the seedling density for other conifers was above the minimum stocking level in all but three of them.

Given trends of increasing fire activity in many forest regions (Westerling, 2016), the area subject to low propagule pressure is likely to expand in the coming decades, while concurrent increases in climatic water deficit would lead to dependence on higher propagule pressure to support a given density of regenerating conifers (Figure 6). Expansion of the area subject to low propagule pressure could arise due to increases in both the rate that mature forest is lost to severe fire in an increasingly arid environment (Barbero et al., 2015; van Mantgem et al., 2013), and the frequency with which high-severity patches are reburned at short intervals, with each successive fire killing most regenerating conifers in the patch interior and some of the older trees along the patch margin (Figure 7). We found that the reduction in postfire seedling density with decreasing propagule pressure was steeper on dry than moist sites (Figure 6), similar to Douglas-fir forests of the northern Rockies (Donato et al., 2016). Thus, as the climate grows increasingly arid (Diffenbaugh et al., 2015; Swain et al., 2016), sites near the dry end of the present distribution of mixed-conifer/mixed-evergreen forests could shift from rapid to protracted recovery following severe fire. Repeated burning could then perpetuate nonforest vegetation in many of these sites

(Odion et al., 2010; Thompson & Spies, 2010; Coop, Parks, McClerman, & Holsinger, 2016; Coppoletta, Merriam, & Collins, 2016; Figure 7), thereby sustaining a lower forest cover across the landscape.

Fire-generated patches of broadleaf trees and shrubs that follow a slow trajectory toward conifer forest recovery were part of the historical landscape in the Klamath and adjacent forest regions (Lauvaux et al., 2016; Nagel & Taylor, 2005; Russell et al., 1998; Wilken, 1967). These patches provide early-seral habitat and contribute to landscape heterogeneity, consistent with many ecological management objectives (Swanson et al., 2011). Thus, we do not recommend a single management strategy aimed at accelerating forest recovery throughout burned landscapes. However, toward the more severe end of potential warming scenarios (RCP 8.5), more than half of the area currently capable of supporting mixed-conifer/mixed-evergreen forest could soon be at risk of poor initial postfire conifer recruitment (Figure 6). In these areas, forest loss to high-severity fire could be nearly irreversible if fire activity increases to the point where these areas are prone to reburn severely before a new conifer canopy develops (Odion et al., 2010; Thompson & Spies, 2010). This study helps identify the portions of the region at greatest risk of such conversion, which could be used to either prioritize targeted management to help prevent certain areas from exceeding their tipping points, or to provide expectations of the degree of landscape transformation likely in the coming decades so that research and management communities can better learn to meet ecological objectives under the changing disturbance and recovery dynamics.

ACKNOWLEDGEMENTS

We are thankful to Chris So, Matthew Davis, Eleanor Pearson, Lily Clarke, Charles Maxwell, Kim Hack, and Dunbar Carpenter for assistance in the field. Bella Reyes, Mary McCabe, Christopher Fernandez, Olivia Christopher, Kate Aldrich, Ruth Cumberland, Thomas Blair, Anna Rollosson, and Maria Wang helped with sample preparation. Rob Pabst, Jeff Shatford, Tom Spies, Carl Skinner, Dan Blessing, Ken Wearstler, Todd Drake, and Patricia Hochhalter provided feedback and logistical support for the field work. Luca Morreale assisted with the climatic water-deficit layers. Jean-Daniel Bontemps provided feedback on the growth models. We are thankful to three anonymous reviewers for their valuable comments. Funding was provided by NSF grant #DEB-1353301.

REFERENCES

- Abatzoglou, J. T., & Williams, A. P. (2016). Impact of anthropogenic climate change on wildfire across western US forests. *Proceedings of the National Academy of Sciences*, 113, 11770–11775.
- Adams, H. D., Guardiola-Claramonte, M., Barron-Gafford, G. A., Villegas, J. C., Breshears, D. D., Zou, C. B., . . . Huxman, T. E. (2009). Temperature sensitivity of drought-induced tree mortality portends increased regional die-off under global-change-type drought. *Proceedings of the National Academy of Sciences*, 106, 7063–7066.
- Allen, C. D., Breshears, D. D., & McDowell, N. G. (2015). On underestimation of global vulnerability to tree mortality and forest die-off from hotter drought in the Anthropocene. *Ecosphere*, 6, 129.

- Anderson-Teixeira, K. J., Miller, A. D., Mohan, J. E., Hudiburg, T. W., Duval, B. D., & DeLucia, E. H. (2013). Altered dynamics of forest recovery under a changing climate. *Global Change Biology*, *19*, 2001–2021.
- Barbero, R., Abatzoglou, J. T., Larkin, N. K., Kolden, C. A., & Stocks, B. (2015). Climate change presents increased potential for very large fires in the contiguous United States. *International Journal of Wildland Fire*, *24*, 892–899.
- Bates, D., Mächler, M., Bolker, B., & Walker, S. (2015). Fitting linear mixed-effects models using lme4. *Journal of Statistical Software*, *67*, 1–48.
- Bontemps, J.-D., & Duplat, P. (2012). A non-asymptotic sigmoid growth curve for top height growth in forest stands. *Forestry*, *85*, 353–368.
- Briles, C. E., Whitlock, C., & Bartlein, P. J. (2005). Postglacial vegetation, fire, and climate history of the Siskiyou Mountains, Oregon, USA. *Quaternary Research*, *64*, 44–56.
- Camp, A., Oliver, C., Hessburg, P., & Everett, R. (1997). Predicting late-successional fire refugia pre-dating European settlement in the Wenatchee Mountains. *Forest Ecology and Management*, *95*, 63–77.
- Carmean, W. H. (1972). Site index curves for upland oaks in the central states. *Forest Science*, *118*, 109–120.
- Chambers, M. E., Fornwalt, P. J., Malone, S. L., & Battaglia, M. A. (2016). Patterns of conifer regeneration following high severity wildfire in ponderosa pine-dominated forests of the Colorado Front Range. *Forest Ecology and Management*, *378*, 57–67.
- Collins, W. J., Bellouin, N., Doutriaux-Boucher, M., Gadney, N., Halloran, P., Hinton, T., ... Woodward, S. (2011). Development and evaluation of an Earth-System model – HadGEM2. *Geoscientific Model Development*, *4*, 1051–1075.
- Colombaroli, D., & Gavin, D. G. (2010). Highly episodic fire and erosion regime over the past 2,000 y in the Siskiyou Mountains, Oregon. *Proceedings of the National Academy of Sciences*, *107*, 18909–18914.
- Coop, J. D., Parks, S. A., McClellan, S. R., & Holsinger, L. M. (2016). Influences of prior wildfires on vegetation response to subsequent fire in a reburned southwestern landscape. *Ecological Applications*, *26*, 346–354.
- Coppoletta, M., Merriam, K. E., & Collins, B. M. (2016). Post-fire vegetation and fuel development influences fire severity patterns in reburns. *Ecological Applications*, *26*, 686–699.
- Daly, C., Conklin, D. R., & Unsworth, M. H. (2010). Local atmospheric decoupling in complex topography alters climate change impacts. *International Journal of Climatology*, *30*, 1857–1864.
- Diffenbaugh, N. S., Swain, D. L., & Touma, D. (2015). Anthropogenic warming has increased drought risk in California. *Proceedings of the National Academy of Sciences*, *112*, 3931–3936.
- Dobrowski, S. Z., Swanson, A. K., Abatzoglou, J. T., Holden, Z. A., Safford, H. D., Schwartz, M. K., & Gavin, D. G. (2015). Forest structure and species traits mediate projected recruitment declines in western US tree species: tree recruitment patterns in the western US. *Global Ecology and Biogeography*, *24*, 917–927.
- Dodson, E. K., & Root, H. T. (2013). Conifer regeneration following stand-replacing wildfire varies along an elevation gradient in a ponderosa pine forest, Oregon, USA. *Forest Ecology and Management*, *302*, 163–170.
- Donato, D. C., Fontaine, J. B., Campbell, J. L., Robinson, W. D., Kauffman, J. B., & Law, B. E. (2009a). Conifer regeneration in stand-replacement portions of a large mixed-severity wildfire in the Klamath-Siskiyou Mountains. *Canadian Journal of Forest Research*, *39*, 823–838.
- Donato, D. C., Fontaine, J. B., Robinson, W. D., Kauffman, J. B., & Law, B. E. (2009b). Vegetation response to a short interval between high-severity wildfires in a mixed-evergreen forest. *Journal of Ecology*, *97*, 142–154.
- Donato, D. C., Harvey, B. J., & Turner, M. G. (2016). Regeneration of montane forests 24 years after the 1988 Yellowstone fires: a fire-catalyzed shift in lower treelines? *Ecosphere*, *7*, e01410.
- Dyer, M. E., & Bailey, R. L. (1987). A test of six methods for estimating true heights from stem analysis data. *Forest Science*, *33*, 3–13.
- ESRI (2015) *ArcGIS 10.4 for desktop*. Redlands, CA: Environmental Systems Research Institute.
- Gergel, D. R., Nijssen, B., Abatzoglou, J. T., Lettenmaier, D. P., & Stumbaugh, M. R. (2017). Effects of climate change on snowpack and fire potential in the western USA. *Climatic Change*, *141*, 287–299.
- Gitelson, A. A., Kaufman, Y. J., Stark, R., & Rundquist, D. (2002). Novel algorithms for remote estimation of vegetation fraction. *Remote Sensing of Environment*, *80*, 76–87.
- Grissino-Mayer, H. D. (2001). Evaluating crossdating accuracy: a manual and tutorial for the computer program COFECHA. *Tree-ring Research*, *57*, 205–221.
- Haire, S. L., & McGarigal, K. (2010). Effects of landscape patterns of fire severity on regenerating ponderosa pine forests (*Pinus ponderosa*) in New Mexico and Arizona, USA. *Landscape Ecology*, *25*, 1055–1069.
- Halofsky, J. E., Donato, D. C., Hibbs, D. E., Campbell, J. L., Cannon, M. D., Fontaine, J. B., ... Spies, T. A. (2011). Mixed-severity fire regimes: lessons and hypotheses from the Klamath-Siskiyou Ecoregion. *Ecosphere*, *2*, art40.
- Harris, R. M. B., Remenyi, T. A., Williamson, G. J., Bindoff, N. L., & Bowman, D. M. J. S. (2016). Climate–vegetation–fire interactions and feedbacks: trivial detail or major barrier to projecting the future of the Earth system? *WIREs Climate Change*, *7*, 910–931.
- Harvey, B. J., Donato, D. C., & Turner, M. G. (2016). High and dry: post-fire tree seedling establishment in subalpine forests decreases with post-fire drought and large stand-replacing burn patches. *Global Ecology and Biogeography*, *25*, 655–669.
- Holz, A., Wood, S. W., Veblen, T. T., & Bowman, D. M. J. S. (2015). Effects of high-severity fire drove the population collapse of the subalpine Tasmanian endemic conifer *Athrotaxis cupressoides*. *Global Change Biology*, *21*, 445–458.
- Hothorn, T., Bretz, F., & Westfall, P. (2008). Simultaneous inference in general parametric models. *Biometrical Journal*, *50*, 346–363.
- Hsu, J. C. (1996). *Multiple Comparisons: Theory and Methods*. New York: Chapman & Hall/CRC Press.
- Jones, C. D., Hughes, J. K., Bellouin, N., Hardiman, S. C., Jones, G. S., Knight, J., ... Zerroukat, M. (2011). The HadGEM2-ES implementation of CMIP5 centennial simulations. *Geoscientific Model Development*, *4*, 543–570.
- Kemp, K. B., Higuera, P. E., & Morgan, P. (2016). Fire legacies impact conifer regeneration across environmental gradients in the U.S. northern Rockies. *Landscape Ecology*, *31*, 619–636.
- Knapp, E. E., Weatherspoon, J., & Skinner, C. N. (2012). Shrub seed banks in mixed conifer forests of northern California and the role of fire in regulating abundance. *Fire Ecology*, *8*, 32–48.
- Lauvaux, C. A., Skinner, C. N., & Taylor, A. H. (2016). High severity fire and mixed conifer forest-chaparral dynamics in the southern Cascade Range, USA. *Forest Ecology and Management*, *363*, 74–85.
- Legates, D. R., & McCabe, G. J. (1999). Evaluating the use of “goodness-of-fit” measures in hydrologic and hydroclimatic model validation. *Water Resources Research*, *35*, 233–241.
- Legates, D. R., & McCabe, G. J. (2013). A refined index of model performance: a rejoinder. *International Journal of Climatology*, *33*, 1053–1056.
- Lintz, H. E., McCune, B., Gray, A. N., & McCulloh, K. A. (2011). Quantifying ecological thresholds from response surfaces. *Ecological Modelling*, *222*, 427–436.
- Lutz, J. A., van Wagtenonk, J. W., & Franklin, J. F. (2010). Climatic water deficit, tree species ranges, and climate change in Yosemite National Park. *Journal of Biogeography*, *37*, 936–950.
- van Mantgem, P. J., Nesmith, J. C. B., Keifer, M., Knapp, E. E., Flint, A., & Flint, L. (2013). Climatic stress increases forest fire severity across the western United States. *Ecology Letters*, *16*, 1151–1156.
- McCune, B. (2006). Non-parametric habitat models with automatic interactions. *Journal of Vegetation Science*, *17*, 819–830.
- McCune, B., & Grace, J. B. (2002). *Analysis of ecological communities*. Gleneden Beach, OR, USA: MjM Software Design. 300 pp.
- McCune, B., & Mefford, M. J. (2009). *HyperNiche. Nonparametric Multiplicative Habitat Modeling. Version 2.30*. Gleneden Beach, OR, USA: MjM Software Design.

- McGinnis, T. W., Shook, C. D., & Keeley, J. E. (2010). Estimating aboveground biomass for broadleaf woody plants and young conifers in Sierra Nevada, California, forests. *Western Journal of Applied Forestry*, 25, 203–209.
- Miller, J. D., Knapp, E. E., Key, C. H., Skinner, C. N., Isbell, C. J., Creasy, R. M., & Sherlock, J. W. (2009). Calibration and validation of the relative differenced Normalized Burn Ratio (RdNBR) to three measures of fire severity in the Sierra Nevada and Klamath Mountains, California, USA. *Remote Sensing of Environment*, 113, 645–656.
- Miller, J. D., Skinner, C. N., Safford, H. D., Knapp, E. E., & Ramirez, C. M. (2012). Trends and causes of severity, size, and number of fires in northwestern California, USA. *Ecological Applications*, 22, 184–203.
- Nagel, T. A., & Taylor, A. H. (2005). Fire and persistence of montane chaparral in mixed conifer forest landscapes in the northern Sierra Nevada, Lake Tahoe Basin, California, USA¹. *Journal of the Torrey Botanical Society*, 132, 442–457.
- Nakagawa, S., & Schielzeth, H. (2013). A general and simple method for obtaining R^2 from generalized linear mixed-effects models. *Methods in Ecology and Evolution*, 4, 133–142.
- NatureServe (2009). *International ecological classification standard: terrestrial ecological classifications*. NatureServe Central Databases: Arlington, VA, USA.
- Odion, D. C., Moritz, M. A., & DellaSala, D. A. (2010). Alternative community states maintained by fire in the Klamath Mountains, USA. *Journal of Ecology*, 98, 96–105.
- Oswald, S. A., Nisbet, I. C. T., Chiaradia, A., & Arnold, J. M. (2012). FlexParamCurve: R package for flexible fitting of nonlinear parametric curves. *Methods in Ecology and Evolution*, 3, 1073–1077.
- Paritsis, J., Veblen, T. T., & Holz, A. (2015). Positive fire feedbacks contribute to shifts from *Nothofagus pumilio* forests to fire-prone shrublands in Patagonia. *Journal of Vegetation Science*, 26, 89–101.
- Pinheiro, J., Bates, D., DebRoy, S., & Sarkar, D., R Core Team (2016) *nlme: Linear and Nonlinear Mixed Effects Models*. R package version 3.1-127, <http://CRAN.R-project.org/packages=nlme>.
- R Core Team (2016). *R: a language and environment for statistical computing*. Vienna, Austria: R Foundation for Statistical Computing.
- Robock, A. (1988). Enhancement of surface cooling due to forest fire smoke. *Science*, 242, 911–913.
- Rogers, B. M., Neilson, R. P., Drapek, R., Lenihan, J. M., Wells, J. R., Bachelet, D., & Law, B. E. (2011). Impacts of climate change on fire regimes and carbon stocks of the U.S. Pacific Northwest. *Journal of Geophysical Research*, 116, G03037.
- Rother, M. T., & Veblen, T. T. (2016). Limited conifer regeneration following wildfires in dry ponderosa pine forests of the Colorado Front Range. *Ecosphere*, 7, e01594.
- Rother, M. T., Veblen, T. T., & Furman, L. G. (2015). A field experiment informs expected patterns of conifer regeneration after disturbance under changing climate conditions. *Canadian Journal of Forest Research*, 45, 1607–1616.
- Russell, W. H., McBride, J., & Rowntree, R. (1998). Revegetation after four stand-replacing fires in the Lake Tahoe basin. *Madrño*, 45, 40–46.
- Serra-Diaz, J. M., Franklin, J., Sweet, L. C., McCullough, I. M., Syphard, A. D., Regan, H. M., ... Davis, F. W. (2016). Averaged 30 year climate change projections mask opportunities for species establishment. *Ecography*, 39, 844–845.
- Shatford, J. P. A., Hibbs, D. E., & Puettmann, K. J. (2007). Conifer regeneration after forest fire in the Klamath-Siskiyou: how much, how soon? *Journal of Forestry*, 105, 139–146.
- Skinner, C. N., Taylor, A. H., & Agee, J. K. (2006). Klamath Mountains Bioregion. In N. G. Sugihara, J. W. van Wagtenonk, J. Fites-Kaufman, K. E. Shaffer, & A. E. Thode (Eds.), *Fire in California's Ecosystems* (pp. 170–194). Berkeley, CA: University of California Press.
- Swain, D. L., Horton, D. E., Singh, D., & Diffenbaugh, N. S. (2016). Trends in atmospheric patterns conducive to seasonal precipitation and temperature extremes in California. *Science Advances*, 2, e1501344.
- Swanson, M. E., Franklin, J. F., Beschta, R. L., Crisafulli, C. M., DellaSala, D. A., Hutto, R. L., ... Swanson, F. J. (2011). The forgotten stage of forest succession: early-successional ecosystems on forest sites. *Frontiers in Ecology and the Environment*, 9, 117–125.
- Tepley, A. J., Swanson, F. J., & Spies, T. A. (2014). Post-fire tree establishment and early cohort development in conifer forests of the western Cascades of Oregon, USA. *Ecosphere*, 5, 80.
- Tepley, A. J., Veblen, T. T., Perry, G. L. W., Stewart, G. H., & Naficy, C. E. (2016). Positive feedbacks to fire-driven deforestation following human colonization of the south island of New Zealand. *Ecosystems*, 19, 1325–1344.
- Thompson, J. R., & Spies, T. A. (2010). Factors associated with crown damage following recurring mixed-severity wildfires and post-fire management in southwestern Oregon. *Landscape Ecology*, 25, 775–789.
- Turner, M. G., Dale, V. H., & Everham, E. H. (1997). Fires, hurricanes, and volcanoes: comparing large disturbances. *BioScience*, 47, 758–768.
- USDA (1989). *Final environmental impact statement, land and resource management plan, Siskiyou National Forest*. Southwest Region: USDA Forest Service Pacific.
- USDA (1995a). *Land and resource management plan, Klamath National Forest (including all amendments as of 7/29/2010)*. Pacific Southwest Region: USDA Forest Service.
- USDA (1995b). *Shasta-trinity national forests, land and resource management plan*. Pacific Southwest Region: USDA Forest Service.
- Westerling, A. L. (2016). Increasing western US forest wildfire activity: sensitivity to changes in the timing of spring. *Philosophical Transactions of the Royal Society B: Biological Sciences*, 371, 20150178.
- Westerling, A. L., & Bryant, B. P. (2008). Climate change and wildfire in California. *Climatic Change*, 87, 231–249.
- Whitlock, C., McWethy, D. B., Tepley, A. J., Veblen, T. T., Holz, A., McGlone, M. S., ... Wood, S. W. (2015). Past and present vulnerability of closed-canopy temperate forests to altered fire regimes: a comparison of the Pacific Northwest, New Zealand, and Patagonia. *BioScience*, 65, 151–163.
- Wilken, G. C. (1967). History and fire record of a timberland brush field in the Sierra Nevada of California. *Ecology*, 48, 302–304.
- Wilkin, K., Ackerly, D., & Stephens, S. (2016). Climate change refugia, fire ecology and management. *Forests*, 7, 77.
- Williams, A. P., Allen, C. D., Macalady, A. K., Griffin, D., Woodhouse, C. A., Meko, D. M., ... McDowell, N. G. (2012). Temperature as a potent driver of regional forest drought stress and tree mortality. *Nature Climate Change*, 3, 292–297.
- Wood, S. N. (2011). Fast stable restricted maximum likelihood and marginal likelihood estimation of semiparametric generalized linear models. *Journal of the Royal Statistical Society Series B (Statistical Methodology)*, 73, 3–36.
- Yamamura, K. (1999). Transformation using $(x + 0.5)$ to stabilize the variance of populations. *Researches on Population Ecology*, 41, 229–234.

SUPPORTING INFORMATION

Additional Supporting Information may be found online in the supporting information tab for this article.

How to cite this article: Tepley AJ, Thompson JR, Epstein HE, Anderson-Teixeira KJ. Vulnerability to forest loss through altered postfire recovery dynamics in a warming climate in the Klamath Mountains. *Glob Change Biol*. 2017; 00: 1–16. <https://doi.org/10.1111/gcb.13704>